https://doi.org/10.2352/ISSN.2470-1173.2020.15.COLOR-349

Developing an inkjet printer IV: printer mechanism control for best print quality*

Daulet Kenzhebalin[1], Baekdu Choi[1], Sige Hu[1], Yin Wang[1], Davi He[2], Zillion Lin[2], George Chiu[1], Jan Allebach[1];
[1] ***School of Electrical and Computer Engineering, Purdue University; West Lafayette, IN;***
[2] ***Sunvalleytek International; Shenzhen, China***

Abstract

Inkjet printer motor control consists of moving the printhead in the scan direction and in the process direction. Both movements have different objectives. Scan direction movement needs to have constant velocity and process direction movement needs to have accurate movement. In this paper, we discuss a method for controlling the velocity of the printhead and how to tune the motor control parameters. We also design six test pages for testing accuracy of the printhead movement and cartridge properties. For each test page, we discuss expected prints, common printer control problems that could alter the print quality, and how to identify them.

Introduction

Inkjet printer motor control consists of moving the printhead in the scan direction and in the process direction. In the scan direction, the printhead goes over the media and drops ink droplets depending on the image and the print mask. In the process direction, the printhead advances to be able to print the rest of the image. The illustration of scan and process directions are shown in Fig. 1. Typical motor control consists of three steps that are repeated until the full image is printed: horizontal movement left to right in the scan direction, horizontal movement right to left in the direction opposite to the scan direction, and movement in the process direction to print the rest of the image. After that, the printhead retraces to a default position. The flowchart is shown in Fig. 2.

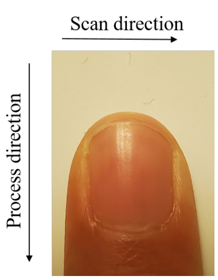

Figure 1. *Illustration of scan and process directions.*

Inkjet printers can print images in different modes depending on the quality and speed desired. If speed is more important than quality, then a 1-pass print mode is used. In 1-pass mode, any row of the image is printed in one horizontal motion. Whereas in 4-pass mode, any row of the image can be printed with 4 different nozzles of the same colorant during 4 different horizontal motions. This usually results in higher quality of the prints. An example of 1-pass and 4-pass prints is shown in Fig. 3. All the images in this paper were printed at 600 dpi and captured by either an Epson 10000XL scanner** or a QEA PIAS-II digital microscope†.

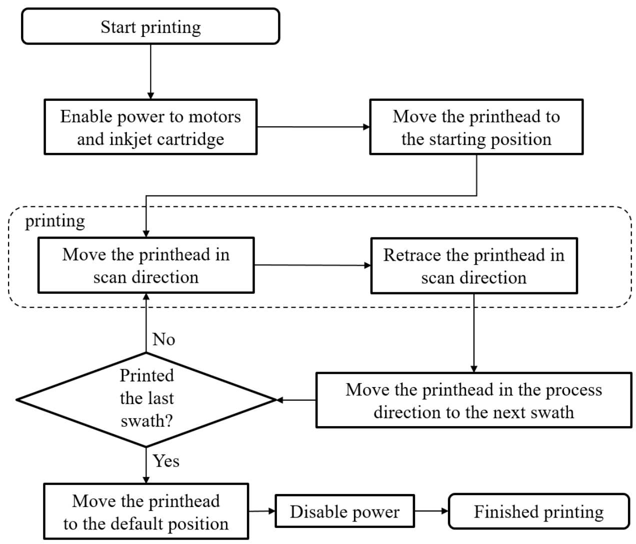

Figure 2. *Printer mechanism control flowchart*

Figure 3. *Comparison of 1-pass and 4-pass print modes. Images are printed in a) 1-pass print mode and b) 4-pass print mode. The images were printed at 600 dpi and scanned at 1200 dpi with an Epson 10000 XL scanner. The width of the original rose image at 600 dpi was about 1 in.*

Kamasak et al. proposed a content-dependent print mode that switched between a 1-pass print mode and a 4-pass print mode depending on the page content [1]. Deshpande et al. de-

*Research supported by Sunvalleytek International, Shenzhen, China.

**Epson America, Inc., Long Beach, CA.
†Quality Engineering Associates Inc., Billerica, MA

scribed the motion control architecture to implement the dynamic print mode [2, 3]. In our printer, the 4-pass print mode has much better print quality compared to the 1-pass mode. In addition, the print zone of our printer is very small, less than 1×1 in^2, and we expect most of the prints to be continuous-tone pictures and graphics rather than text. Therefore, we decided to use a 4-pass print mode.

The printhead movement in the process direction is simpler than the movement in the scan direction. The most important requirement for the movement in the process direction is distance precision. That is, it is important that the printhead move the same distance from swath to swath. Therefore, a stepper motor is utilized for the process direction movement of the printhead.

The printhead movement in the scan direction needs to have a constant velocity when the printhead is in the printing zone (over the media). If the velocity is not constant, then the distance between the ink droplets will not be constant due to acceleration and deceleration of the printhead. This usually results in banding artifacts. An example of a print with a banding artifact is shown in Fig. 4.

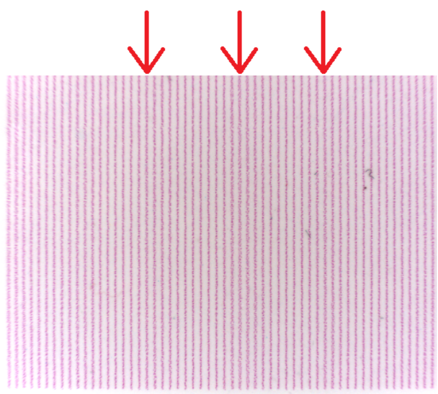

Figure 4. *Example of banding artifacts due to non-constant velocity. The arrows point to the locations of the dark bands. The motor control was chosen to result in a small velocity oscillation. The image was printed at 600 dpi and captured at 1021 dpi using a QEA PIAS-II digital microscope.*

Measuring velocity

Velocity is measured using an optical encoder. The optical encoder has a resolution of 600 dpi and has 2 digital outputs. Depending on the position of the printhead the outputs can be either {0,0}, {0,1}, {1,0}, or {1,1}, where 1 is high voltage output and 0 is low voltage output. The optical encoder is located on the top of the printhead. Using the optical encoder, the microcontroller can decode the movement direction and keep track of the position of the printhead. The decode logic is summarized in the Fig. 5. Depending on the current state and the previous state, the direction of the motor movement can be decoded as being +1 (in the scan direction) or -1 (opposite to the scan direction). The state transition is shown with arrows. Note that due to the design of the optical encoder, both channels cannot switch their output states at the same time.

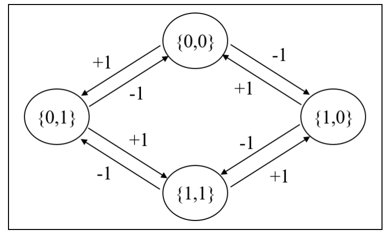

Figure 5. *Direction decoder for 2 channel optical encoder. Each channel has a binary output: 0 or 1. Depending on the current state and the previous state, the direction of the motor movement can be decoded as being +1 (in the scan direction) or -1 (opposite to the scan direction). The state transition is shown with arrows.*

DC motor control

For the cartridge movement in the scan direction we use a DC motor. The DC motor is controlled by a motor driver TI DRV8801. The main characteristic for good motor control in the scan direction is the speed consistency. Speed consistency ensures that ink droplets will be evenly spaced. Otherwise, the prints may have banding artifacts. We implemented a PID controller for speed control.

PID controller

The input to a DC motor is controlled by PWM (pulse width modulation) output from a microcontroller. Parameters of PWM are frequency and the duty cycle. Varying the duty cycle results in varying voltage inputs to the DC motor. We chose a frequency of 26.6 kHz. This frequency is beyond the range of audible frequencies for humans, and is just below the input limit for the motor driver.

The output duty cycle is computed using a PID controller [4]. PID stands for proportional-integral-derivative. First, the error term is computed between the reference velocity and the measured velocity. Then, the integral and derivative terms are computed. The integral term is the summation of all error terms. The derivative term is the difference between the current error and the previous error. Finally, the duty cycle is computed using the three computed terms and the three coefficients (K_p, K_i, K_d) that need to be tuned. The equations are shown in Eqs. 1 - 4.

$$e[n] = V_{reference}[n] - V_{measured}[n], \tag{1}$$

$$i[n] = i[n-1] + e[n], \tag{2}$$

$$d[n] = e[n] - e[n-1], \tag{3}$$

$$out[n] = K_p e[n] + K_i i[n] + K_d d[n], \tag{4}$$

where $e[n]$ is the error term, $i[n]$ is the integral term, $d[n]$ is the derivative term, and $out[n]$ is the output duty cycle. The tuning of the PID coefficients is described in the next subsection.

Tuning the PID coefficients

Tuning the PID coefficients is done in three steps. First, we set $K_i = K_d = 0$, so that the derivative and integral terms do not contribute anything to the output duty cycle. This way, the K_p coefficient can be optimized. Fig. 6 shows the effect of varying the K_p coefficient. Higher K_p coefficients lead to velocities that are close to the reference velocity. Lower K_p coefficients lead to velocities with less oscillation and less overshoot. $K_p = 0.1$ has the velocity profile with the least standard deviation. We chose this value, since the standard deviation was judged to be acceptably low; and there was no overshoot after the initial acceleration zone at around 0.01 ms.

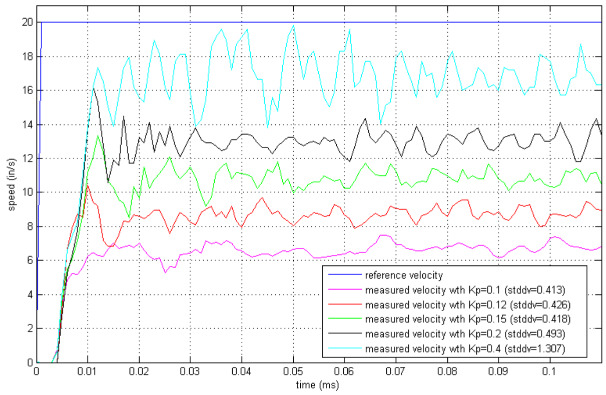

Figure 6. *Comparison of speed consistency using only the error term with varying K_p coefficients ($K_i = K_d = 0$). The reference velocity is 20 in/s. Higher K_p coefficients lead to velocities that are close to the reference velocity and higher overshoot at 0.01 ms. Lower K_p coefficients lead to velocities with less oscillation.*

Next, using the K_p coefficient obtained earlier, we find the optimal K_i coefficient. Fig. 7 shows the effect of varying the K_i coefficient. $K_p = 0.1$ and $K_i = 0.01$ produce the velocity profile with the least MSE. Here, we use a different metric to compare the performance of the chosen coefficients. MSE (mean squared error) can be used in this case because the desired velocity can be achieved with the integral coefficient as opposed to the tuning of the K_p coefficient. When tuning the K_p coefficient, we only look at the velocity variation because the desired velocity cannot be achieved with $K_i = 0$.

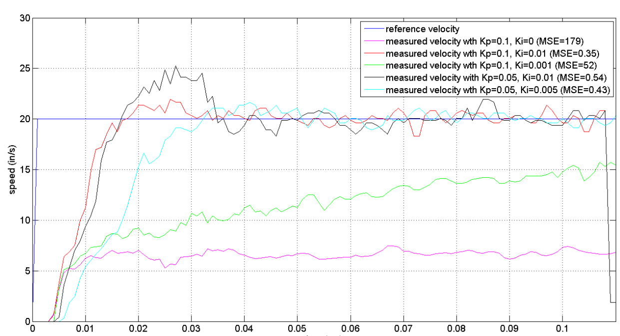

Figure 7. *Comparison of speed consistency using the error and the integral terms with varying K_p and K_i coefficients ($K_d = 0$). The reference velocity is 20 in/s. $K_p = 0.1$ and $K_i = 0.01$ produce the velocity with the least oscillation (measured in terms of MSE in the interval 0.04 s − 0.1 s).*

Lastly, we tune the K_d coefficient. Fig. 8 shows the effect of varying the K_d coefficient with $K_p = 0.1$ and $K_i = 0.01$. Adding the derivative term higher than 0.001 increases the MSE. Therefore, K_d was chosen to be 0.001. As a final check, this experiment was repeated with varying K_p, K_i, and K_d coefficients. As a result, the set of tuned coefficients are summarized in Eqs. 5-7.

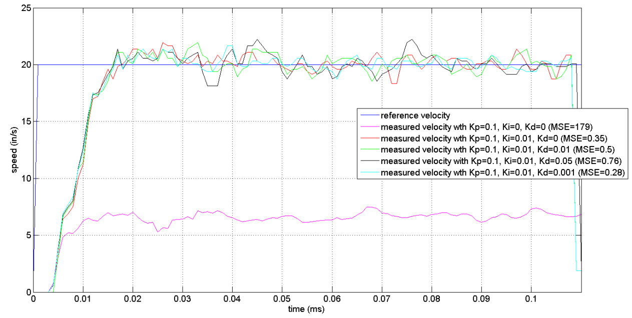

Figure 8. *Comparison of speed consistency using all 3 terms with varying K_d coefficient. The reference velocity is 20 in/s. $K_d = 0.001$ produces the velocity with the least oscillation (measured in terms of MSE in the interval 0.04 s − 0.1 s).*

$$K_p = 0.1 \tag{5}$$

$$K_i = 0.01 \tag{6}$$

$$K_d = 0.001 \tag{7}$$

After adjusting the parameters, we reprinted the image with banding artifacts that was shown in the introduction section. The resulting images are shown in Fig. 9.

Optimization for PID controller on a microcontroller

The PID controller can be optimized to have better performance on the microcontroller. We added two improvements. First, we initialize the integral term to a large number. This is done so that the motor starts moving earlier. With duty cycle outputs lower than 60%, the motor doesn't move at all due to the load mass. Therefore, we initialized the integral term at the beginning of PID controller to have the following value.

$$i[0] = \frac{60}{K_i} \tag{8}$$

Another optimization we added was to change the multiplication by the PID coefficients to integer division. To implement this, we found the inverse of the coefficients obtained earlier and performed integer division on the microcontroller. The velocity performance of the PID controller with integer division was identical to the PID controller with floating point division, but the time spent in the interrupt routine was cut from 200 μs to 45 μs. This is significant because at the velocity of 20 in/s with the optical encoder resolution of 600 dpi, the interrupt period from the optical encoder is around 83 μs. With integer division, the duty cycle can be updated once per every optical encoder interrupt. With floating point division, the duty cycle can be updated only once per 3 optical encoder interrupts.

Test images

In order to verify that the printer mechanism is working properly, we designed several different test images. Before printing these test images, we needed to verify that the nozzles were functional and weren't clogged. Therefore, we designed a test image for easily testing every nozzle. This test image is shown in Fig. 10. The image consists of vertical and horizontal line segments. Each horizontal line segment is supposed to be printed with one nozzle. This is done so that the user can clearly identify the malfunction of nozzles by verifying the presence of all horizontal line segments. Therefore, it is preferred to use one-pass mode. The nozzle test can also be performed with multi-pass mode, but a special print mask needs to be designed. Vertical lines are used for separating horizontal lines which correspond to different nozzles. If some of the horizontal line segments are missing, then the nozzle cleaning needs to be performed.

There are 4 rows of 16 horizontal line segments for each colorant. Each horizontal line segment is 2 pixels higher than the horizontal line segment to the left and 2 pixels lower than the horizontal line segment to the right. The nozzles for each colorant are arranged in two staggered columns. The odd-numbered nozzles are in the left column; and the even-numbered nozzles are in the right column. With this arrangement in mind, the layout of the test page can be interpreted as follows: the top 2 rows correspond to odd nozzles; and the bottom 2 rows correspond to even nozzles. The nozzles corresponding to the leftmost horizontal line segment in each row of cyan horizontal line segments are 33, 1, 34, 2. In

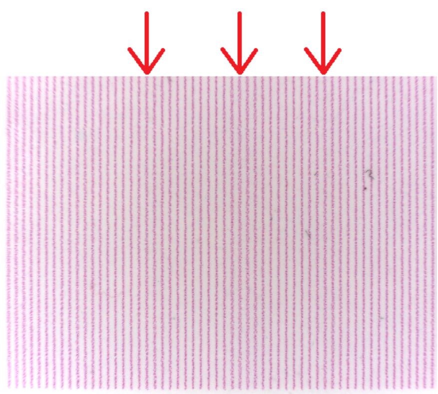

a)

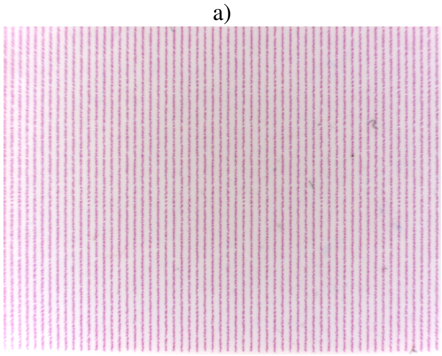

b)

Figure 9. *Example illustrating the effect of the velocity profile on print quality (Test Page 1). The image consists of single pixel wide lines of magenta color that are 10 pixels apart. The image was printed in bi-directional mode. Note that the image in a) has vertical banding artifacts (The arrows point to the locations of the dark bands.), which are not present in the image in b). a) image printed with parameters that yield oscillating velocity profile. b) image printed with tuned parameters. The images were printed at 600 dpi and captured at 1021 dpi using a QEA PIAS-II digital microscope.*

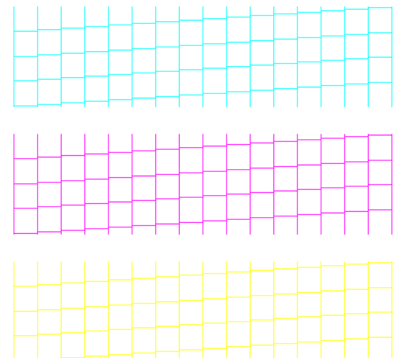

a)

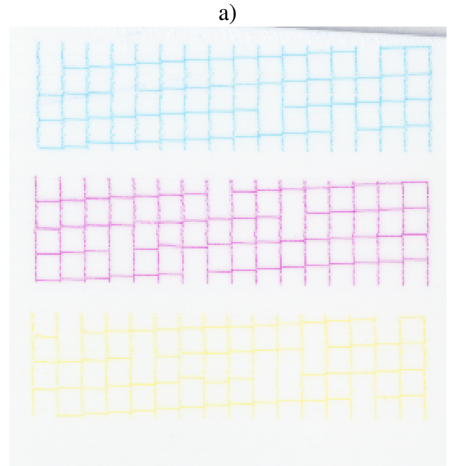

b)

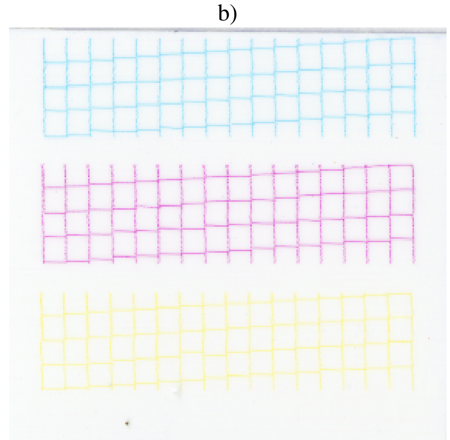

c)

Figure 10. *Nozzle test image and examples of prints (Test Page 2): a) test image to be printed; b) example of print with clogged nozzles; c) example of print with all clean nozzles. There are a total of 192 horizontal line segments which correspond to 192 nozzles in the cartridge. Each horizontal line segment will be printed with one of the 192 nozzles. If a line segment is missing, then the corresponding nozzle is clogged. The images were printed at 600 dpi and scanned at 1200 dpi with an Epson 10000 XL scanner.*

Fig. 10 b) cyan nozzles 7, 33, 59, 26, 52 are clogged.

We also designed an image for testing the process direction movement. The image consists of black horizontal lines. The spacing between the lines is chosen to be the number of pixels in a swath, so that each line is printed with the same combination of cyan, magenta, and yellow nozzles. If all three color lines fall on top of each other, the step size of the AC motor and the spacing between different colorant nozzles is chosen properly. Fig. 11 shows a test image and two different sample prints. The images were printed in 2-pass print mode. The print with incorrect step size has a lot of single-color horizontal lines. In the print with the correct step size, single-color horizontal lines are placed on top of each other to create a composite black line as expected.

a)

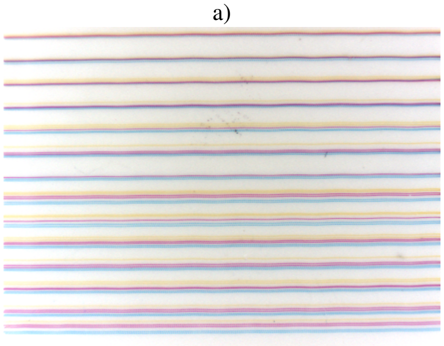

b)

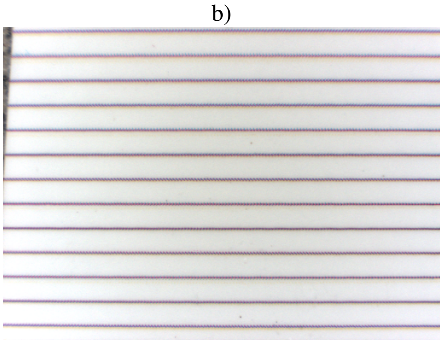

c)

Figure 11. *Process direction movement test 1 (Test Page 3): a) test image; b) sample print with the incorrect (smaller) step size c) sample print with the correct step size. The images were printed in a 2-pass print mode. The images were printed at 600 dpi and captured at 1021 dpi using a QEA PIAS-II digital microscope.*

In order to further test the consistency of the process direction movement, we designed another test page shown in Fig. 12. This test image consists of single-color horizontal lines. The spacing between lines is 12 pixels, which is the swath height when printing in 4-pass mode. The print mask for this image consists of all 1's, which implies that all the lines in this image will be printed in the 1st pass and with the same nozzle. After printing the test page, the print is scanned at 1200 dpi resolution. Then, we extract line positions using Otsu's method [5] and connected components [6]. The full flowchart is shown in Fig. 13.

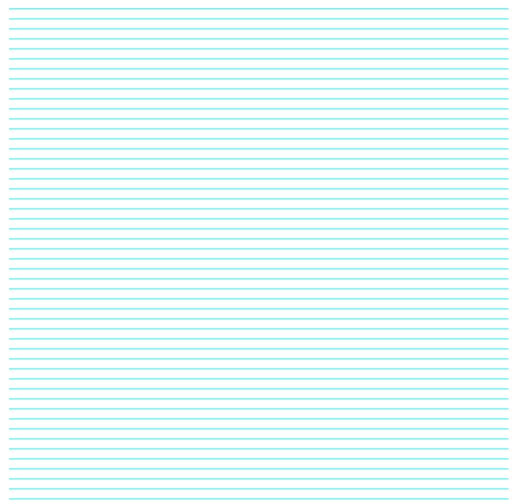

a)

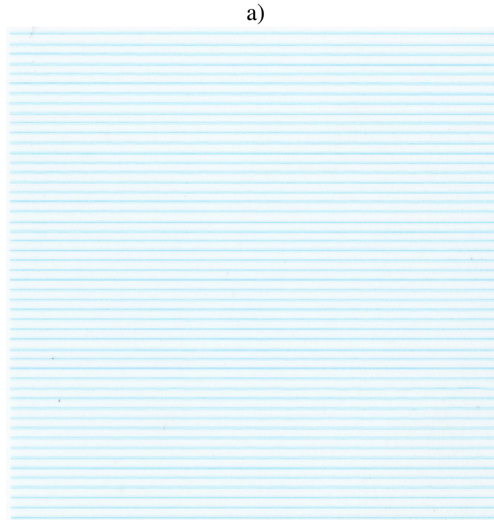

b)

Figure 12. *Process direction movement test 2 (Test Page 4): a) test image; b) sample print result. The spacing between the lines is equal to swath height and the print mask should consist of only 1's. All the lines in the image will be printed with one nozzle making it easy to analyze the movement. The image was printed at 600 dpi and scanned at 1200 dpi with an Epson 10000 XL scanner.*

After extracting the line positions, we compute the line-to-line distances and plot them as shown in Fig. 14. There are 2 swath movements have an error of more than the spacing between two adjacent nozzles (1/600 in). All other swath movements have error less than or equal to 1/600 in. This error was judged to be acceptable.

Another important parameter is the distance between columns of even and odd nozzles. In order to verify that this parameter is correctly implemented, we designed the test page shown in Fig. 15. Each row consists of 5 columns of even nozzles followed by 5 columns of odd nozzles and alternating afterwards. The difference between each row is that the columns of odd nozzles are shifted by 1 or 2 pixels to the left or to the right. In the first row, the odd nozzles are shifted to the left by 2 pixels. In the second row, the odd nozzles are shifted to the left by 1 pixel. In the third row, the odd nozzles are not shifted. Therefore, this row looks the smoothest in the test image. In the fourth row, the odd nozzles are shifted to the right by 1 pixel. In the fifth row, the odd nozzles are shifted to the right by 2 pixels. If the alignment is correct, then the 3rd row of the print should be the smoothest. Fig. 15 shows a sample test result. In this example, the second row is the smoothest. But it is only slightly smoother than the third row. So we concluded that the alignment between even and odd columns of nozzles was acceptable.

The last test image checks the alignment between different colorants. The test image is shown in Fig. 16. The test image has 5 rows. Each row is made up of the same magenta, yellow, and cyan dots superimposed on top of each other. The difference between the rows is that the yellow and cyan dots are shifted up and down relative to the magenta dots by either 2 or 4 pixels. In the middle row, all magenta, yellow, and cyan dots are on top of each other resulting in composite black dots. In the 2nd row from the top, the yellow dots are shifted 2 pixels up and cyan dots are shifted 2 pixels down relative to the magenta dots. As a result of this shifting, the top dots are yellow, followed by red (yel-

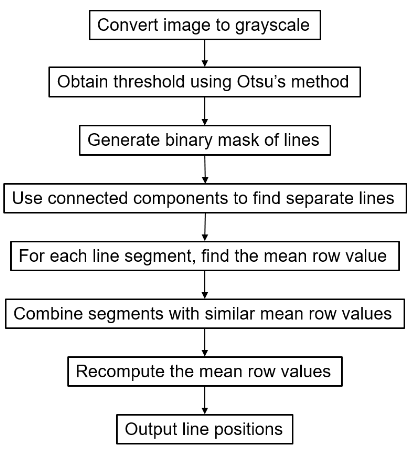

Figure 13. *Line position extraction flowchart.*

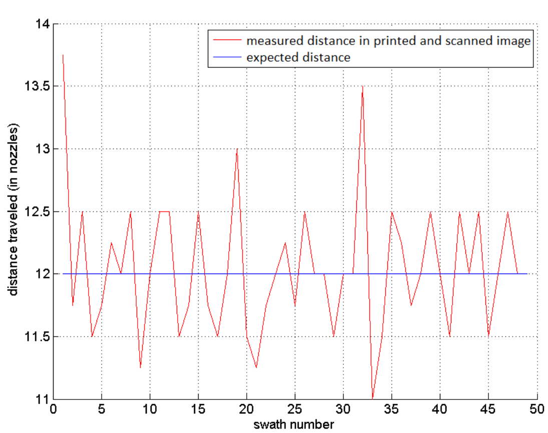

Figure 14. *The distance measured between consecutive horizontal lines shown in Fig.12 b). The process direction distance between adjacent nozzles is 1/600 in.*

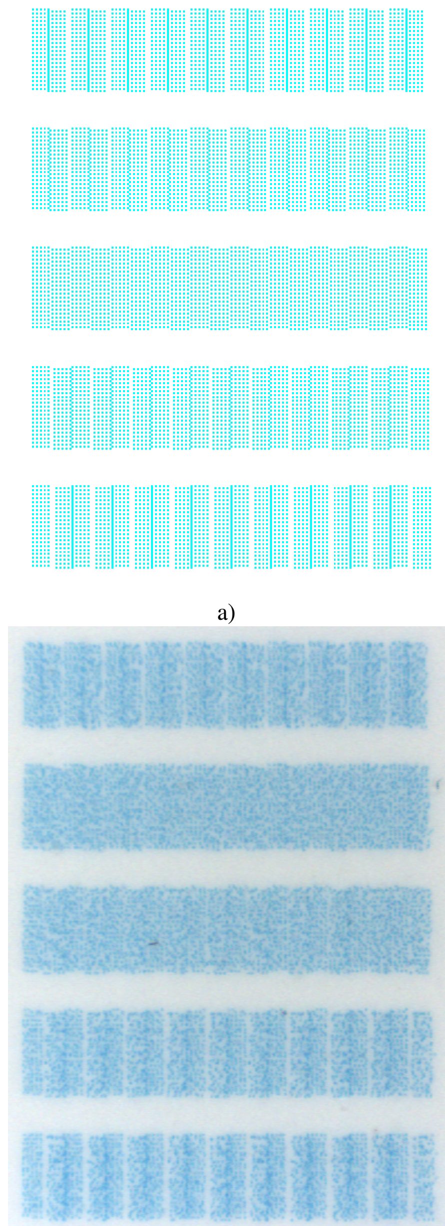

b)

Figure 15. *Test of alignment between columns of even and odd nozzles (Test Page 5): a) test image; b) sample printed and scanned image. If the alignment is correct, the middle row (3rd) should be the smoothest. In this example, the second row is the smoothest. But it is only slightly smoother than the third row. So we concluded that the alignment between even and odd columns of nozzles was acceptable. The image was printed at 600 dpi and captured at 1021 dpi using a QEA PIAS-II digital microscope.*

low+magenta), followed by black (yellow+magenta+cyan), followed by blue (magenta+cyan), followed by cyan dots on the bottom. The three other rows are designed similarly. If the 3rd row of the print doesn't have any outlines on top and bottom, then the alignment is good. Fig. 16 shows the results for a sample printed and scanned image. In this sample, all of the rows, except the 3rd row, clearly show clear non-black dots on the outline. Therefore, we can conclude that the printer has a good alignment between colorants.

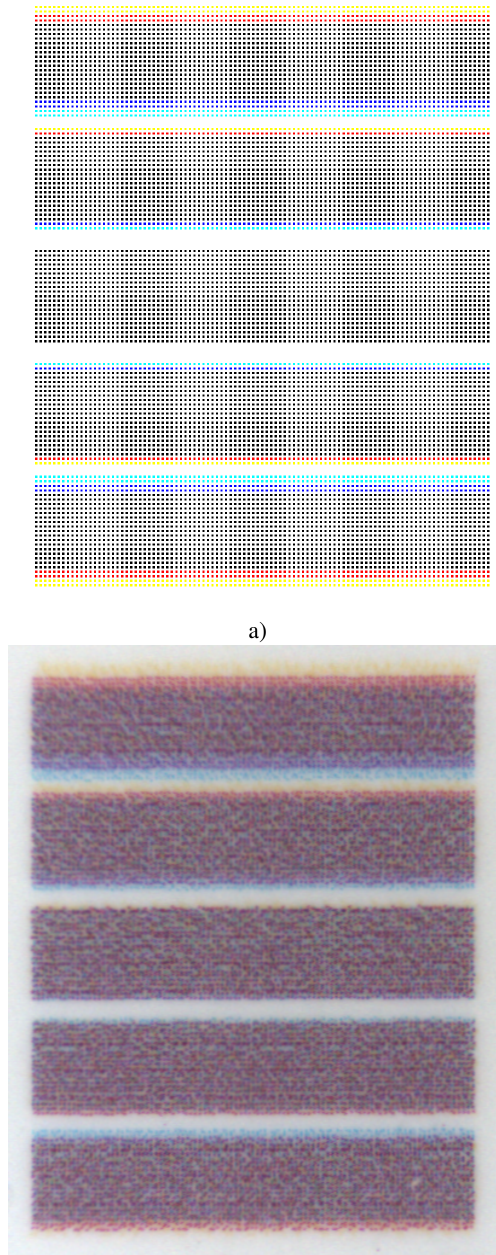

a)

b)

Figure 16. *Test of alignment between colorants (Test Page 6): a) test image; b) sample printed and scanned image. If the alignment is correct, then the middle row (3rd) should not have any visible yellow, magenta or cyan outlines as in the test image. In this example, the 3rd row of the printed image does not have visible outlines, so the printer has a good alignment between colorants. The image was printed at 600 dpi and captured at 1021 dpi using a QEA PIAS-II digital microscope.*

Conclusion

In this paper, we introduced the main parts of the motor control for inkjet printers. The most important requirements for the motor control were discussed, such as constant velocity for scan direction and the precise distance for process direction. The full procedure was implemented on an inkjet printer. The constant velocity in the process direction was achieved by using a PID controller. The method of tuning the parameters for the PID controller was discussed and supported with examples. To verify that the controller works well for printing, an image was printed with the tuned parameters. The resulting image has a good print quality and doesn't have banding artifacts which are usually caused by various motor control issues. We also designed five additional test images for testing different aspects of the printer mechanism and cartridge. Some images were designed so that the results can be interpreted visually. One test requires doing image processing of the scanned print. We described the sample prints and common issues.

References

[1] M. Kamasak, A. V. Deshpande, K. L. Thoon, C. A. Bouman, G. T. Chiu, and J. P. Allebach, "Dynamic print modes for inkjet printing," in IS& T NIP-17 Int. Conf. Digital Printing Technol., Ft. Lauderdale, FL, Sep. 2001, pp. 78-82.

[2] A. V. Deshpande, M. Kamasak, K. L. Thoon, G. T. Chiu, C. A. Bouman, J. P. Allebach, S. Fedigan, D. Schafer, and C. Cole, "Design and implementation of a dsp based inkjet printer motion control system for dynamic print mode control," in IS& T NIP-17 Int. Conf. Digital Printing Technol., Ft. Lauderdale, FL, Sep. 2001, pp. 34-42.

[3] A. V. Deshpande, M. Kamasak, K. L. Thoon, G. T. Chiu, C. A. Bouman, J. P. Allebach, S. Fedigan, D. Schafer, and C. Cole, "Development of an inkjet carriage motion controller for dynamic print mode control," in 2nd IFAC Conf. Mechatronic Syst., Berkeley, CA, Dec. 2002, doi: 10.1016/S1474-6670(17)33976-9.

[4] M. A. Johnson and M. H. Moradi, PID control. London, UK: Springer-Verlag London Limited, 2005.

[5] N. Otsu, "A Threshold Selection Method from Gray-Level Histograms." IEEE Transactions on Systems, Man, and Cybernetics. Vol. 9, No. 1, 1979, pp. 62–66.

[6] R. M. Haralick, and L. G. Shapiro, Computer and Robot Vision, Volume I, Addison-Wesley, 1992, pp. 28-48.

Author Biography

Daulet Kenzhebalin received his BS in computer engineering from Purdue University (2015). Currently he is pursuing a PhD in electrical engineering at Purdue University. His primary area of research has been image processing and machine learning.

Baekdu Choi received his B.Sc. in electrical and computer engineering from Seoul National University, Seoul, South Korea in 2017 and is currently working on a Ph.D. in electrical and computer engineering at Purdue University, West Lafayette, IN, USA. His research mainly focuses on digital image processing,

digital halftoning and color management for inkjet printers.

Sige Hu received his BS in Electrical and Computer Engineering from Pennsylvania State University (2017) and is currently pursuing PhD in Electrical and Computer Engineering at Purdue University. His research is mainly focus on image processing.

Yin Wang received her B.S.(2016) in Electrical Engineering from Purdue University. She currently is a Ph.D candidate at Purdue University EISL (Electronic and Imaging System Laboratory) supervised by Professor Jan. P. Allebach. Her research focuses on color image processing, computer vision, 3D reconstruction and deep learning application.

Peng(Davi) He is a software manager in Sunvalleytek International Inc, Shenzhen, Guangdong, China. He received his BS in Communication Engineering from Hunan University of Arts and Science, Changde, Hunan, China in 2012. His current research interest including artificial intelligence and robot.

Zillion(Zhenqing) Lin is a technical director in Sunvalleytek International Inc, Shenzhen, Guangdong, China. He received his BS in Microelectronics Engineering from University of Electronic Science and Technology of China, Chengdu, Sichuan, China in 2008 and MS in Biomedical Engineering from Shenzhen University, Shenzhen, Guangdong, China. His current research interest including artificial intelligence and robot.

George T. Chiu is a Professor in the School of Mechanical Engineering with courtesy appointments in the School of Electrical and Computer Engineering and the Department of Psychological Sciences at Purdue University. He also serves as the Assistant Dean for Global Engineering Programs and Partnership for the College of Engineering. Dr. Chiu received the B.S. degree in Mechanical Engineering from the National Taiwan University in 1985 and the M.S. and Ph.D. degrees in Mechanical Engineering from the University of California at Berkeley, in 1990 and 1994, respectively. From September 2011 to June 2014, he served as the Program Director for the Control Systems Program at the National Science Foundation. His current research interests are mechatronics and dynamic systems and control with applications to digital printing and imaging systems, digital fabrications and functional printing, human motor control, motion and vibration perception and control. He received the 2012 NSF Director's Collaboration Award and the 2010 IEEE Transactions on Control System Technology Outstanding Paper Award. He served as the Editor-in-Chief for the IEEE/ASME Transactions on Mechatronics from 2017-19 and as the Editor for the Journal of Imaging Science and Technology from 2012-14. Dr. Chiu served on the Executive Committee of the ASME Dynamic Systems and Control Division (DSCD) from 2007 to 2014 and as the Chair of the Division from 2012-13. He is a Fellow of ASME and a Fellow of the Society for Imaging Science and Technology (IS&T).

Jan P. Allebach is Hewlett-Packard Distinguished Professor of Electrical and Computer Engineering at Purdue University. Allebach is a Fellow of the IEEE, the National Academy of Inventors, the Society for Imaging Science and Technology (IS&T), and SPIE. He was named Electronic Imaging Scientist of the Year by IS&T and SPIE, and was named Honorary Member of IS&T, the highest award that IS&T bestows. He has received the IEEE Daniel E. Noble Award and the IS&T/OSA Edwin Land Medal, and is a member of the National Academy of Engineering.